

Enhancement of a reduced order doubly fed induction generator model for wind farm transient stability analyses

Mehmet Kenan DÖŞOĞLU^{1,*}, Ayşen BASA ARSOY²

¹Electrical & Electronics Engineering Department, Faculty of Technology, Düzce University, Düzce, Turkey

²Electrical Engineering Department, Faculty of Engineering, Kocaeli University, Kocaeli, Turkey

Received: 18.02.2014

Accepted/Published Online: 05.07.2014

Final Version: 15.04.2016

Abstract: Dynamic modeling of a doubly fed induction generator (DFIG) implemented for wind power systems is very important for transient stability. The rotor dynamic model (RDM) as well as the reduced order model (ROM) of a DFIG has been developed for transient analysis purpose. The performances of reduced order DFIG models with/without RDM have been compared. Modeling and analyses have been carried out in MATLAB/SIMULINK. Comparison of system behaviors against 3 phase fault is made between without RDM and with RDM. Several parameters such as output voltage, active power, speed, electrical torque variations, and d-q axis stator and rotor current variations of the DFIG along with a 34.5 kV bus voltage have been examined. In addition, the responses of DFIG output voltage and electrical torque have been compared for the cases of full order and reduced order DFIG models with rotor dynamics. It has been seen that the system becomes stable in a short time when the rotor dynamic is included in a reduced order DFIG model.

Key words: Doubly fed induction generator (DFIG), reduced order model (ROM), rotor dynamic modeling (RDM), transient stability

1. Introduction

Renewable energy sources have taken an important role in electrical energy generation due to recent escalating prices and limited usage of fossil fuels. Wind power is the fastest growing and penetrating source among renewables. Nowadays, DFIG wind turbines are the most widely emerging technology used for wind power generation. They can provide high efficiency, better control of active power and torque, and improved power quality [1,2]. High penetration of wind power into a power system may lead to serious concern about its influence on system stability. Accurate dynamic modeling is therefore important to analyze the interaction between the power system and large wind power plants. Simplified models are preferred to reduce the model order, numerical integration, and the computation time by neglecting stator transients in transient stability analyses [3–6]. Many studies have investigated the modeling issue. An equivalent model for DFIG wind plants has been developed [7] by aggregating the wind turbines in a wind farm into a single equivalent turbine to represent the whole wind power plant. This simplified model showed a good performance under both normal operation and grid disturbance while reducing the order model and computation time. The performance of reduced order modeling has been tested in another study [8] along with control and protection schemes. Power system disturbances have been considered as network voltage sag, three phase faults, and voltage instability. The effect of neglecting stator transients in the DFIG model has been discussed [9] under the cases of subsynchronous and supersynchronous

*Correspondence: kenan_33@hotmail.com

speed, validating the use of the reduced order DFIG model from the transient stability point of view. The work presented in [10] compares three reduced order DFIG models and shows that the second order model can represent the system dynamics very well during normal operating conditions. While control schemes have been developed for rotor side and grid side converters of DFIG using a reduced order DFIG model [11], the study conducted [12] demonstrates that a four quadrant AC-AC converter connected to the rotor windings of the DFIG can increase the transient stability margin of the grid; therefore, the behavior of the DFIG is more robust in the event of critical faults.

Determination of control parameters in the DFIG is important for system stability. The effects of turbine and system parameters on voltage stability are emphasized in [13] and [14]. In the analysis, a model of a wind turbine with a DFIG and its associated controllers is indicated, and a small signal stability model is derived [15,16]. DFIG output voltage and frequency should be within the limits required by standards and the grid code. Control strategies for voltage and short time frequency regulation are essential to comply with wind power connection requirements [17,18].

While rotor dynamics are considered in [19] on a full order DFIG model, this study proposes including rotor dynamics on a reduced order DFIG model and therefore developing an enhanced reduced order DFIG model. The developed model has been tested against three phase faults on a sample system. Simulation results have been compared with the results obtained from the model without rotor dynamics. Some simulation results have also been discussed for the cases of both a full and reduced order DFIG model.

2. Components of doubly fed induction generators

DFIG wind turbines use a wound rotor induction generator, where the rotor winding is fed through a grid side converter and a rotor side converter as shown in Figure 1.

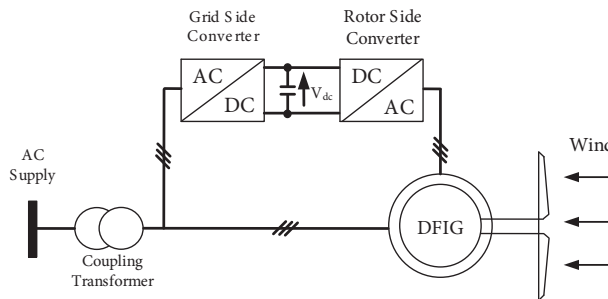


Figure 1. DFIG circuit model.

The function of the grid side inverter is to balance the DC link voltage and to provide reactive power compensation, while the rotor side inverter controls stator side the real and reactive power of the DFIG. Voltage limits and an over-current “crowbar” circuit protect the machine and converters [20].

In modeling the DFIG, the full order model is represented by four equations, considering the generator’s variables in the d-q synchronous reference frame. The equations for the stator and rotor windings can be written as follows [21]:

$$\begin{bmatrix} v_{ds} \\ v_{qs} \end{bmatrix} = \begin{bmatrix} R_s & 0 \\ 0 & R_s \end{bmatrix} \begin{bmatrix} i_{ds} \\ i_{qs} \end{bmatrix} + w_s \begin{bmatrix} 0 & -1 \\ 1 & 0 \end{bmatrix} \begin{bmatrix} \lambda_{ds} \\ \lambda_{qs} \end{bmatrix} + \begin{bmatrix} \dot{\lambda}_{ds} \\ \dot{\lambda}_{qs} \end{bmatrix} \quad (1)$$

$$\begin{bmatrix} v_{dr} \\ v_{qr} \end{bmatrix} = \begin{bmatrix} R_r & 0 \\ 0 & R_r \end{bmatrix} \begin{bmatrix} i_{dr} \\ i_{qr} \end{bmatrix} + s\omega_s \begin{bmatrix} 0 & -1 \\ 1 & 0 \end{bmatrix} \begin{bmatrix} \lambda_{dr} \\ \lambda_{qr} \end{bmatrix} + \begin{bmatrix} \dot{\lambda}_{dr} \\ \dot{\lambda}_{qr} \end{bmatrix} \quad (2)$$

Flux-inductance equations can be expressed in the d-q synchronous frame as follows:

$$\begin{bmatrix} \lambda_{ds} \\ \lambda_{qs} \end{bmatrix} = \begin{bmatrix} L_s + L_m & 0 \\ 0 & L_s + L_m \end{bmatrix} \begin{bmatrix} i_{ds} \\ i_{qs} \end{bmatrix} + \begin{bmatrix} L_m & 0 \\ 0 & L_m \end{bmatrix} \begin{bmatrix} i_{dr} \\ i_{qr} \end{bmatrix} \quad (3)$$

$$\begin{bmatrix} \lambda_{dr} \\ \lambda_{qr} \end{bmatrix} = \begin{bmatrix} L_m & 0 \\ 0 & L_m \end{bmatrix} \begin{bmatrix} i_{ds} \\ i_{qs} \end{bmatrix} + \begin{bmatrix} L_r + L_m & 0 \\ 0 & L_r + L_m \end{bmatrix} \begin{bmatrix} i_{dr} \\ i_{qr} \end{bmatrix}, \quad (4)$$

where i_{ds} , i_{qs} , i_{dr} , i_{qr} : d and q axis currents of stator and rotor, L_s and L_r : inductance of stator and rotor, L_m : magnetizing inductance. L_{ss} and L_{rr} can be written in terms of stator mutual inductance and rotor mutual inductance as given in (5) and (6).

$$L_{ss} = L_m + L_s \quad (5)$$

$$L_{rr} = L_m + L_r \quad (6)$$

A reduced order model of a DFIG is employed to simplify the relationship between the steady state variable and the outputs of the DFIG. The simplified model can enable us to easily predict the behavior of the DFIG under transient conditions. In this model, a stator is represented by transient induced voltages behind a transient reactance where stator fluxes are neglected. The main idea is that the dc component is omitted from the stator transient current. Electrical equations describing stator side in the reduced order model of the machine are given below:

$$\begin{bmatrix} v_{ds} \\ v_{qs} \end{bmatrix} = \begin{bmatrix} R_s & 0 \\ 0 & R_s \end{bmatrix} \begin{bmatrix} i_{ds} \\ i_{qs} \end{bmatrix} + \begin{bmatrix} 0 & -X' \\ X' & 0 \end{bmatrix} \begin{bmatrix} i_{ds} \\ i_{qs} \end{bmatrix} + \begin{bmatrix} e_d \\ e_q \end{bmatrix} \quad (7)$$

$$\begin{bmatrix} \dot{e}_d \\ \dot{e}_q \end{bmatrix} = -\frac{1}{T_0} \left\{ \begin{bmatrix} e_d \\ e_q \end{bmatrix} \pm \begin{bmatrix} 0 & X - X' \\ X - X' & 0 \end{bmatrix} \begin{bmatrix} i_{ds} \\ i_{qs} \end{bmatrix} \right\} \pm \omega_s \begin{bmatrix} 0 & s \\ s & 0 \end{bmatrix} \begin{bmatrix} e_d \\ e_q \end{bmatrix} \quad (8)$$

$$\pm \omega_s \begin{bmatrix} 0 & \frac{L_m}{L_{ss}} \\ \frac{L_m}{L_{ss}} & 0 \end{bmatrix} \begin{bmatrix} v_{dr} \\ v_{qr} \end{bmatrix}$$

In these equations, v_{ds} , v_{qs} , v_{dr} , v_{qr} : d and q axis voltages of stator and rotor, $\lambda_{ds}, \lambda_{qs}, \lambda_{dr}, \lambda_{qr}$: d and q axis magnetizing fluxes of stator and rotor, e_d , e_q : d and q axis source voltages of stator, ω_s : synchronous speed, s : slip, r_s , r_r resistance of stator and rotor, stator reactance. Stator reactance (X) and transient reactance (X') of the model is expressed in Eqs. (9)–(10), while transient open circuit time constant (T_0) is given in Eq. (11) [22].

$$X = \omega_s(L_m + L_s) \quad (9)$$

$$X' = w_s \left((L_m + L_s) - \frac{L_m^2}{L_m + L_r} \right) \quad (10)$$

$$T_0 = \frac{L_r + L_m}{R_r} \quad (11)$$

3. Enhanced DFIG rotor dynamic modeling (RDM)

The reduced order DFIG model can be enhanced by including rotor dynamic modeling. It is intended to provide dynamic control of both sides by adding induced voltages on the rotor axis in addition to the transient reactance and the induced voltages used for neglecting the rate of change of stator flux linkage in the reduced order stator model. The change of the ROM can be derived by ignoring the differential term in Eq. (1). Then stator voltages can be written as follows:

$$\begin{bmatrix} v_{ds} \\ v_{qs} \end{bmatrix} = \begin{bmatrix} R_s & 0 \\ 0 & R_s \end{bmatrix} \begin{bmatrix} i_{ds} \\ i_{qs} \end{bmatrix} + w_s \begin{bmatrix} 0 & -1 \\ 1 & 0 \end{bmatrix} \begin{bmatrix} \lambda_{ds} \\ \lambda_{qs} \end{bmatrix} \quad (12)$$

Rotor d-q axis currents derived from Eq. (4) can be substituted in Eq. (2); then the following rotor voltage equations can be obtained:

$$\begin{aligned} \begin{bmatrix} v_{dr} \\ v_{qr} \end{bmatrix} &= \begin{bmatrix} R_r & 0 \\ 0 & R_r \end{bmatrix} \begin{bmatrix} i_{dr} \\ i_{qr} \end{bmatrix} + \begin{bmatrix} 0 & -sw_s \\ sw_s & 0 \end{bmatrix} \left\{ \begin{bmatrix} L_r + L_m & 0 \\ 0 & L_r + L_m \end{bmatrix} \begin{bmatrix} i_{dr} \\ i_{qr} \end{bmatrix} + \begin{bmatrix} L_m & 0 \\ 0 & L_m \end{bmatrix} \begin{bmatrix} i_{ds} \\ i_{qs} \end{bmatrix} \right\} \\ &+ \begin{bmatrix} L_r + L_m & 0 \\ 0 & L_r + L_m \end{bmatrix} \begin{bmatrix} \dot{i}_{dr} \\ \dot{i}_{qr} \end{bmatrix} + \begin{bmatrix} L_m & 0 \\ 0 & L_m \end{bmatrix} \begin{bmatrix} \dot{i}_{ds} \\ \dot{i}_{qs} \end{bmatrix} \end{aligned} \quad (13)$$

From Eq. (3), stator d-q axis currents can be written in terms of stator flux linkage and rotor d-q axis currents as given in Eq. (14), and taking the derivative of the stator currents as seen in Eq. (15):

$$\begin{bmatrix} i_{ds} \\ i_{qs} \end{bmatrix} = \begin{bmatrix} \frac{1}{L_s + L_m} & 0 \\ 0 & \frac{1}{L_s + L_m} \end{bmatrix} \begin{bmatrix} \lambda_{ds} \\ \lambda_{qs} \end{bmatrix} - \begin{bmatrix} \frac{L_m}{L_s + L_m} & 0 \\ 0 & \frac{L_m}{L_s + L_m} \end{bmatrix} \begin{bmatrix} i_{dr} \\ i_{qr} \end{bmatrix} \quad (14)$$

$$\begin{bmatrix} \dot{i}_{ds} \\ \dot{i}_{qs} \end{bmatrix} = \begin{bmatrix} \frac{L_m}{L_m + L_s} & 0 \\ 0 & \frac{L_m}{L_m + L_s} \end{bmatrix} \begin{bmatrix} \dot{i}_{dr} \\ \dot{i}_{qr} \end{bmatrix} \quad (15)$$

Eqs. (14) and (15) can be substituted in Eq. (13). Then the following rotor voltage equation can be obtained. After some rearrangements, the rotor voltages can be written as given in Eq. (19).

$$\begin{aligned} \begin{bmatrix} v_{dr} \\ v_{qr} \end{bmatrix} &= \begin{bmatrix} R_r & 0 \\ 0 & R_r \end{bmatrix} \begin{bmatrix} i_{dr} \\ i_{qr} \end{bmatrix} + \begin{bmatrix} 0 & -sw_s L_m \\ sw_s L_m & 0 \end{bmatrix} \begin{bmatrix} \frac{1}{L_s + L_m} & 0 \\ 0 & \frac{1}{L_s + L_m} \end{bmatrix} \begin{bmatrix} \lambda_{ds} \\ \lambda_{qs} \end{bmatrix} \\ &- \begin{bmatrix} \frac{L_m}{L_s + L_m} & 0 \\ 0 & \frac{L_m}{L_s + L_m} \end{bmatrix} \begin{bmatrix} \dot{i}_{dr} \\ \dot{i}_{qr} \end{bmatrix} \end{aligned}$$

$$\begin{aligned}
& + \begin{bmatrix} 0 & -sw_s(L_r + L_m) \\ sw_s(L_r + L_m) & 0 \end{bmatrix} \begin{bmatrix} i_{dr} \\ i_{qr} \end{bmatrix} + \begin{bmatrix} \frac{L_m^2}{L_s + L_m} & 0 \\ 0 & \frac{L_m^2}{L_s + L_m} \end{bmatrix} \begin{bmatrix} \dot{i}_{dr} \\ \dot{i}_{qr} \end{bmatrix} \\
& + \begin{bmatrix} L_r + L_m & 0 \\ 0 & L_r + L_m \end{bmatrix} \begin{bmatrix} \dot{i}_{dr} \\ \dot{i}_{qr} \end{bmatrix} - \begin{bmatrix} R_r & 0 \\ 0 & R_r \end{bmatrix} - \begin{bmatrix} 0 & \frac{-sw_s L_m}{L_s + L_m} \\ \frac{sw_s L_m}{L_s + L_m} & 0 \end{bmatrix} \\
& + \begin{bmatrix} 0 & -sw_s(L_r + L_m) \\ sw_s(L_r + L_m) & 0 \end{bmatrix} \begin{bmatrix} i_{dr} \\ i_{qr} \end{bmatrix} + \begin{bmatrix} \frac{L_m^2}{L_s + L_m} + L_r + L_m & 0 \\ 0 & \frac{L_m^2}{L_s + L_m} + L_r + L_m \end{bmatrix} \begin{bmatrix} \dot{i}_{dr} \\ \dot{i}_{qr} \end{bmatrix} \\
& + \begin{bmatrix} 0 & \frac{-sw_s L_m}{L_s + L_m} \\ \frac{sw_s L_m}{L_s + L_m} & 0 \end{bmatrix} \begin{bmatrix} \lambda_{ds} \\ \lambda_{qs} \end{bmatrix}
\end{aligned} \tag{16}$$

where

$$L_{r1} = -\frac{L_m}{L_s + L_m} + L_r + L_m \tag{17}$$

$$L_{r2} = \frac{L_m}{L_s + L_m} + L_r + L_m \tag{18}$$

$$\begin{aligned}
\begin{bmatrix} v_{dr} \\ v_{qr} \end{bmatrix} & = \begin{bmatrix} R_r & 0 \\ 0 & R_r \end{bmatrix} \begin{bmatrix} i_{dr} \\ i_{qr} \end{bmatrix} + L_{r1} \begin{bmatrix} 0 & -sw_s \\ sw_s & 0 \end{bmatrix} \begin{bmatrix} i_{dr} \\ i_{qr} \end{bmatrix} + \begin{bmatrix} L_{r2} & 0 \\ 0 & L_{r2} \end{bmatrix} \begin{bmatrix} \dot{i}_{dr} \\ \dot{i}_{qr} \end{bmatrix} \\
& + \begin{bmatrix} 0 & \frac{-sw_s L_m}{L_s + L_m} \\ \frac{sw_s L_m}{L_s + L_m} & 0 \end{bmatrix} \begin{bmatrix} \lambda_{ds} \\ \lambda_{qs} \end{bmatrix}
\end{aligned} \tag{19}$$

The last term in the equation can be represented by rotor voltage source.

$$\begin{bmatrix} E_d \\ E_q \end{bmatrix} = \begin{bmatrix} 0 & \frac{-sw_s L_m}{L_s + L_m} \\ \frac{sw_s L_m}{L_s + L_m} & 0 \end{bmatrix} \begin{bmatrix} \lambda_{ds} \\ \lambda_{qs} \end{bmatrix} \tag{20}$$

The angular speed based on stator flux under normal operating conditions of the DFIG is stable. However, in the transient case angular speed changes. According to the basic flux rule, the drop of voltage in output voltage of the DFIG does not change the flux instantaneously. Therefore, the stator flux ratio in the drop of 3 phase voltage produces dc-component. This component has been seen as an oscillator during the transfer in synchronous reference frame and it is used as stator time constant at the same time. The stator flux change during the voltage drop is shown in Eq. (21).

$$\lambda_{sdq0} = \left\{ \begin{array}{l} \lambda_{sdq0} \cong \frac{v_{sdq0}}{w_s} \\ \lambda_{sdq2} + (\lambda_{sdq0} - \lambda_{sdq2})e^{-\sigma t} e^{-w_s t} \end{array} \right\} \tag{21}$$

Based on Eq. (21) and neglecting stator resistance and flux, equivalent rotor source voltage can be described with the following equation:

$$E_{sdq0} = \left\{ \begin{array}{l} \frac{L_m}{L_{ss}} s \lambda_{sdq0} \\ \frac{L_m}{L_{ss}} s \lambda_{sdq2} - \frac{L_m}{L_{ss}} (1 - s) (\lambda_{sdq0} - \lambda_{sdq2}) e^{-\sigma t} e^{-w_s t} \end{array} \right\} \tag{22}$$

Here λ_{sdq0} and λ_{sdq2} are the steady and transient stator flux linkage, respectively, v_{sdq0} is steady stator d-q axis voltage, t is the time, and σ is the stator damping coefficient given in Eq. (23).

$$\sigma = 1 - \frac{L_m}{L_s L_r} \quad (23)$$

In Eq. (21), the first line refers to the pre-transient status and the second line refers to the stator flux after transient status. The stator flux has been shown in two parts: before and after the voltage drop. These two parts are controlled by the rotor d-q axis induced voltages. In Eq. (22), the term of $(L_m/L_{ss})/s\lambda_{sdq0}$ provides the control as in the 1st part, and the sliding rate of rotor E_{dq} voltage in transient status is small. In the 2nd part, the rotor has been used to protect the converter circuit in the rotor side from the overcurrent and long-term unstable status [19,23].

4. Simulation study

A 2.3 MW wind power system depicted in Figure 2 is used to study the transient behavior of the wind turbine grid interaction.

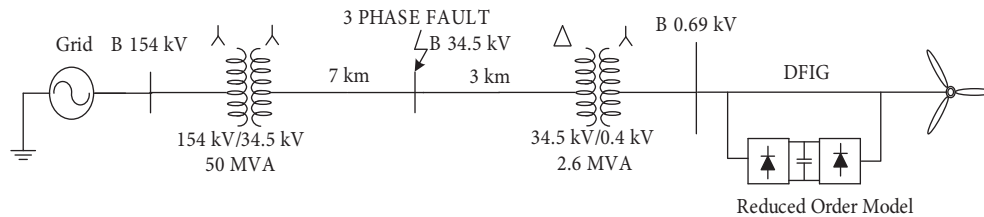


Figure 2. Simulated test system.

The wind turbine generator is represented by two models: reduced order DFIG model and enhanced reduced order DFIG model as explained in the previous section. The wind power plant is connected to a 34.5 kV system through a 2.6 MW, 0.69 kV Y/34.5 kV Δ transformer. There is 10 km distance between the plant and the 154 kV substation. A 50 MW 34.5 kV Y/154 kV Y transformer provides the transmission grid connection. Wind speed is considered to be 8 m/s constant. Saturation of transformers is neglected. In the DFIG, stator resistance of 0.00706 ohm, rotor resistance of 0.005 ohm, stator inductance of 0.171 henry, rotor inductance of 0.156 henry, and inertia constant of 3.5 s have been selected as generator parameters [19]. An enhanced RDM is formed in the MATLAB/SIMULINK environment as given in Figure 3.

5. Simulation study results

A three phase fault has been considered as a transient disturbance in this study. The fault was applied at the B34.5 bus shown in Figure 2, starting at 0.56 s and ending at 0.58 s. The 34.5 kV bus DFIG output voltage during the fault has been shown in Figures 4 and 5.

This is conducted for the 34.5 kV bus voltage and DFIG's output voltage. As expected, less oscillatory behavior has been observed in the case of the enhanced reduced order DFIG model. The response of the DFIG active power is illustrated in Figure 6.

Once the fault is cleared, the active power has oscillations with large variations in the case of the reduced order DFIG model. However, the enhanced model results in the same amount of active power following little oscillations.

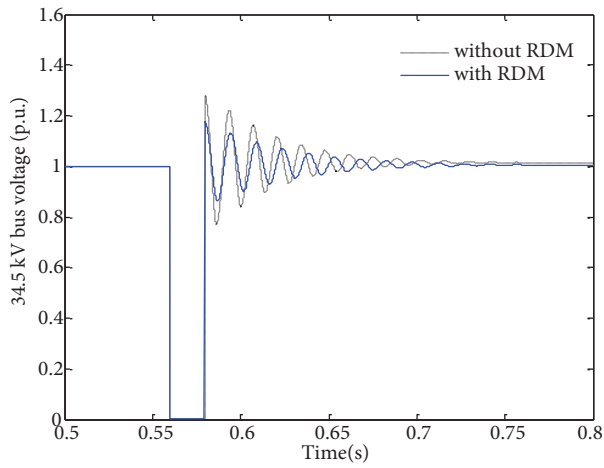


Figure 4. 34.5 kV bus voltage variations.

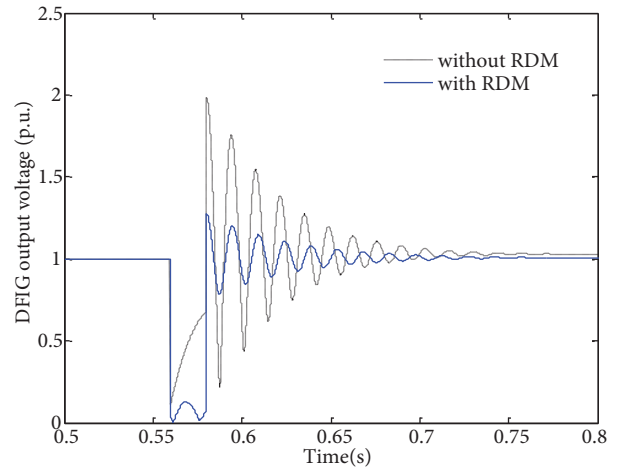


Figure 5. DFIG output voltage variations.

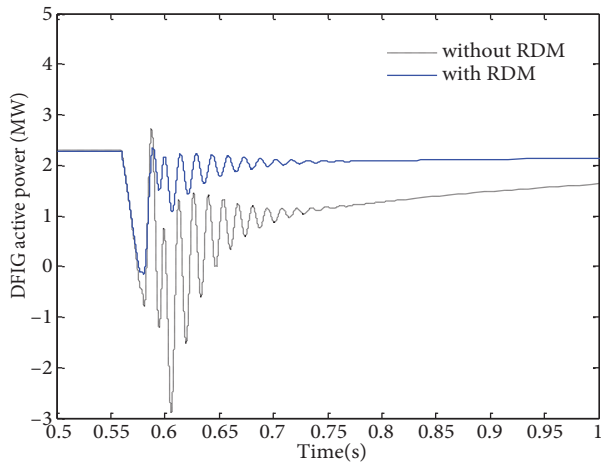


Figure 6. DFIG active power variations.

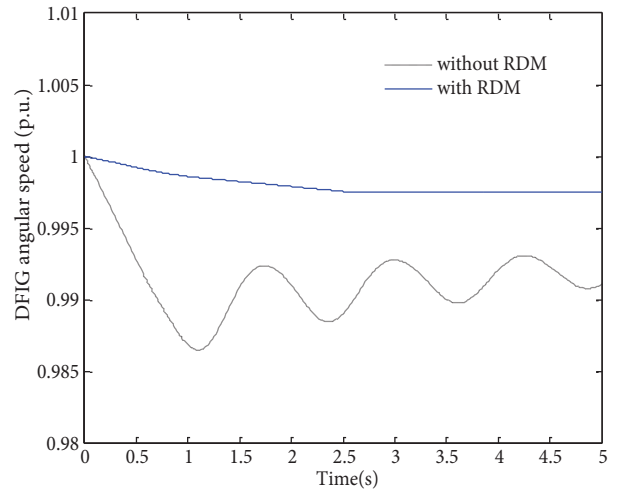


Figure 7. DFIG angular speed variations.

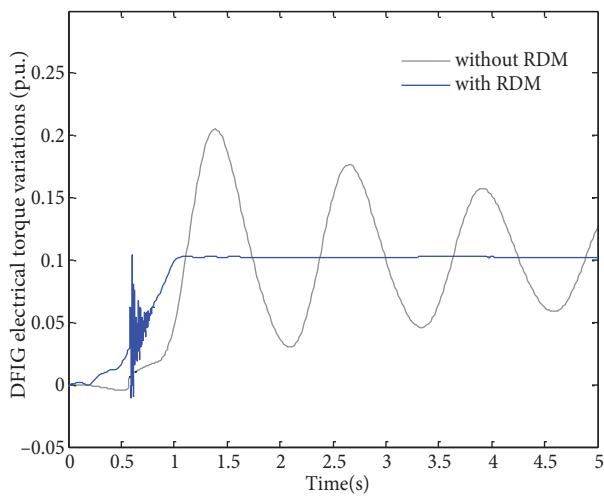


Figure 8. DFIG electrical torque variations.

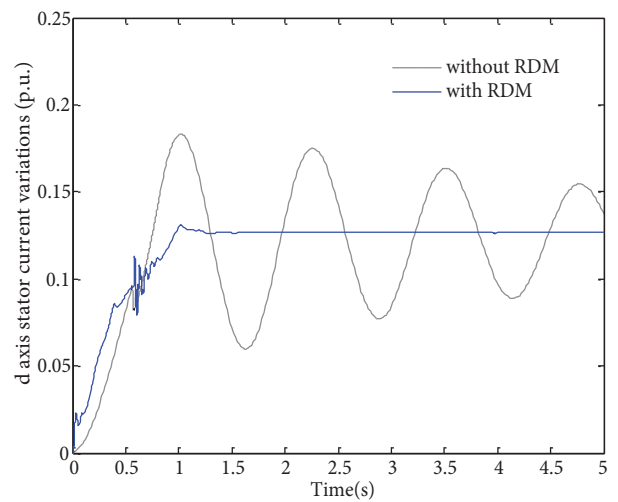


Figure 9. DFIG d axis stator current variations.

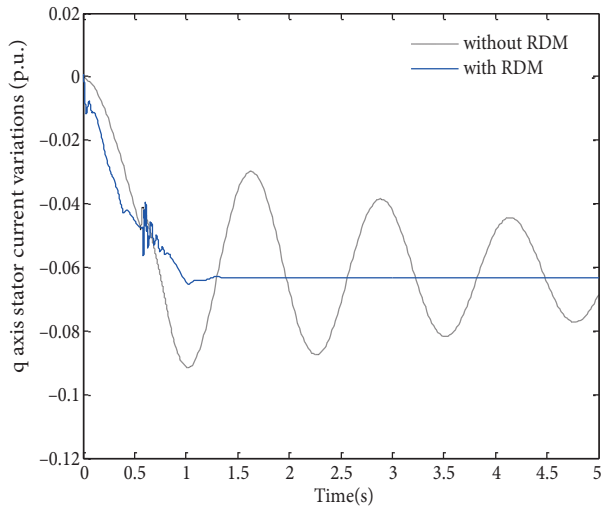


Figure 10. DFIG q axis stator current variations.

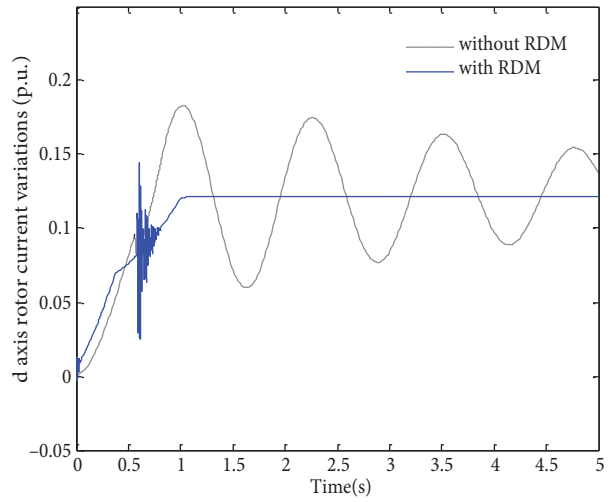


Figure 11. DFIG d axis rotor current variations.

In this period, the speed and electrical torque variation response shows no oscillatory behavior, and d-q axis stator and rotor current variations are better when the DFIG model includes rotor dynamic. As can be seen from the analysis results, voltage swings are damped within a second in both cases. However, variations in other parameters such as active power, angular speed, and d-q axis current last longer when no RDM exists. In Figures 6 and 7, there seems to be a difference between steady state values of active power and angular speed of the two models. This is because of the time axis selected to be short for better focusing on the transient interval. Actually, steady state values for the two models reach the same values in a longer period of time.

Previous analyses have been carried out to show the transient response of a reduced order DFIG model with rotor dynamics. As the reduced order DFIG model is a simplified model, the response of the full order DFIG model with RDM has also been compared with the reduced model ones as given in Figures 13 and 14.

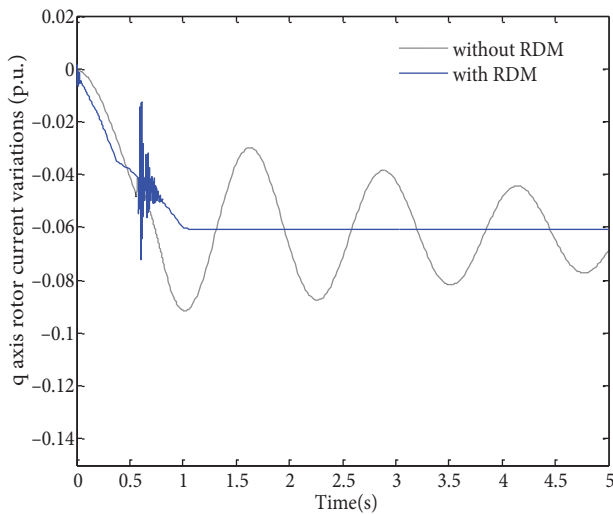


Figure 12. DFIG q axis rotor current variations.

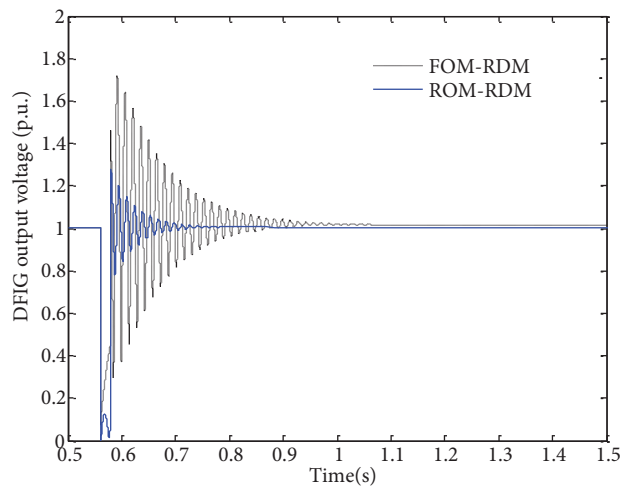


Figure 13. DFIG output voltage variations (FOM-RDM and ROM-RDM).

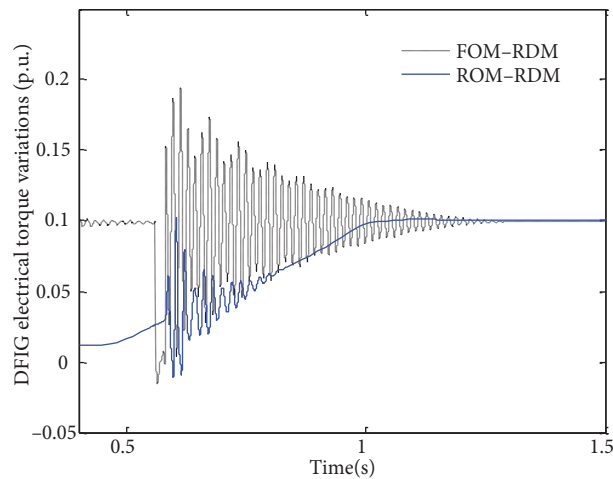


Figure 14. DFIG electrical torque variations (FOM-RDM and ROM-RDM).

This is conducted for the DFIG's output voltage and electrical torque. As expected, less oscillatory behavior has been observed in the case of the enhanced reduced order DFIG model.

6. Conclusion

A ROM with rotor dynamic has been proposed in this paper. The equations for the enhanced model have been derived. Transient responses of this model with the classical reduced order DFIG model have been compared by observing several DFIG parameters such as DFIG output voltage, active power, angular speed, electrical torque, stator, and rotor d-q axes current. Simulation results have shown that oscillations in all parameters are reduced with the use of the enhanced reduced order DFIG model. Including rotor dynamic has a great effect on stator currents, active power, and speed variation by damping oscillations in a very short time. The impact of rotor dynamics in both the full and reduced order DFIG models against a transient case has also been examined in this paper. The enhanced reduced order DFIG model has shown less oscillatory behavior when subjected to a three phase fault. Therefore, the transient stability of a grid connected wind power plant can be improved by taking rotor dynamics into account in the reduced order DFIG model.

References

- [1] Chen JZ, Spooner E. Grid power quality with variable speed wind turbine. *IEEE T Energy Convers* 2001; 16: 148-154.
- [2] Lobos T, Rezmer J, Sikorski T, Waclawek Z. Power distortion issues in wind turbine power systems under transient states. *Turk J Electr Eng & Comp Sci* 2008; 16: 229-238.
- [3] Ekanayake JB, Holdsworth L, Jenkins N. Comparison of 5th order and 3rd order machine models for doubly fed induction generator (DFIG) wind turbines. *Electr Pow Syst Res* 2003; 67: 207-215.
- [4] Ramtharan G, Jenkins N, Anaya-Lara O. Modelling and control of synchronous generators for wide-range variable-speed wind turbines. *Wind Energy* 2007; 10: 231-246.
- [5] Hansen AD, Michalke G. Fault ride-through capability of DFIG wind turbines. *Renew Energy* 2007; 32: 1594-1610.
- [6] García-Gracia M, Comech MP, Sallán J, Llombart A. Modelling wind farms for grid disturbance studies. *Renew Energy* 2008; 33: 2109-2121.
- [7] Fernandez LM, Garcia CA, Saenz JR, Jurado F. Equivalent models of wind farms by using aggregated wind turbines and equivalent winds. *Energy Convers Manage* 2009; 50: 691-704.

- [8] Holdsworth L, Wu XG, Ekanayake JB, Jenkins N. Comparison of fixed speed and doubly-fed induction wind turbines during power system disturbances. *IET Gener Transm Distrib* 2003; 150: 343-352.
- [9] Ledesma P, Usaola J. Effect of neglecting stator transients in doubly fed induction generators models. *IEEE T Energy Convers* 2004; 19: 459-461.
- [10] Sørensen P, Hansen AD, Lund T, Bindner H. Reduced models of doubly fed induction generator system for wind turbine simulations. *Wind Energy* 2006; 9: 299-311.
- [11] Erlich I, Kretschmann J, Fortmann J, Mueller-Engelhardt S, Wrede H. Modeling of wind turbines based on doubly-fed induction generators for power system stability studies. *IEEE T Pow Syst* 2007; 22: 909-919.
- [12] Nunes MV, Lopes JP, Zurn HH, Bezerra UH, Almeida RG. Influence of the variable-speed wind generators in transient stability margin of the conventional generators integrated in electrical grids. *IEEE T Energy Convers* 2004; 19: 692-701.
- [13] Ostadi A, Yazdani A, Varma RK. Modeling and stability analysis of a DFIG-based wind-power generator interfaced with a series-compensated line. *IEEE T Pow Deliv* 2009; 24: 1504-15414.
- [14] Dusonchet L, Telaretti E. Effects of electrical and mechanical parameters on the transient voltage stability of a fixed speed wind turbine. *Electr Pow Syst Res* 2011; 81: 1308-1316.
- [15] Rouco L, Zamora JL. Dynamic patterns and model order reduction in small-signal models of doubly fed induction generators for wind power applications. In: *IEEE Power Engineering Society General Meeting*; 23–28 June 2006; Montreal, Canada. pp. 1-8.
- [16] Wu F, Zhang XP, Godfrey K, Ju P. Small signal stability analysis and optimal control of a wind turbine with doubly fed induction generator. *IET Gener Transm Distrib* 2007; 1: 751-760.
- [17] Cartwright P, Holdsworth L, Ekanayake JB, Jenkins N. Co-ordinated voltage control strategy for a doubly-fed induction generator (DFIG)-based wind farm. *IET Gener Transm Distrib* 2004; 151: 495-502.
- [18] Anaya-Lara O, Hughes FM, Jenkins N, Strbac G. Contribution of DFIG-based wind farms to power system short-term frequency regulation. *IET Gener Transm Distrib* 2006; 153: 164-170.
- [19] Rahimi M, Parniani M. Efficient control scheme of wind turbines with doubly fed induction generators for low-voltage ride-through capability enhancement. *IET Renew Pow Gener* 2010; 4: 242-252.
- [20] Xu L. Enhanced control and operation of DFIG-based wind farms during network unbalance. *IEEE T Energy Convers* 2008; 23: 1073-1081.
- [21] Krause PC, Oleg W, Scott DS. *Analysis of electric machinery and drive systems*. Piscataway, NJ, USA: IEEE Press, 2002.
- [22] Lei Y, Mullane A, Lightbody G, Yacamini R. Modeling of the wind turbine with a doubly fed induction generator for grid integration studies. *IEEE T Energy Convers* 2006; 21: 257-264.
- [23] Guo W, Xiao L, Dai S. Enhancing low-voltage ride-through capability and smoothing output power of DFIG with a superconducting fault-current limiter–magnetizing energy storage system. *IEEE T Energy Convers* 2010; 27: 277-295.